



# Sensitivity analysis of P-wave reflection coefficients for horizontal transverse isotropy (HTI) media

Pedro Canhaço, Igor Braga, Renzo Francia and Uilli Freitas, Invision Geophysics, Brazil

Copyright 2019, SBGf - Sociedade Brasileira de Geofísica

This paper was prepared for presentation during the 16<sup>th</sup> International Congress of the Brazilian Geophysical Society held in Rio de Janeiro, Brazil, 19-22 August 2019.

Contents of this paper were reviewed by the Technical Committee of the 16<sup>th</sup> International Congress of the Brazilian Geophysical Society and do not necessarily represent any position of the SBGf, its officers or members. Electronic reproduction or storage of any part of this paper for commercial purposes without the written consent of the Brazilian Geophysical Society is prohibited.

## Abstract

Characterization and development of reservoirs, which the set of fractures and in situ stress play a key role, is an important exploration problem faced by researchers currently. As seismic data is one of the most relevant sources of information in reservoir studies, the variation analysis of P-wave reflection coefficients with azimuth (AVAz analysis) in a horizontal transverse isotropic (HTI) media shows that anisotropic effects change the AVO response and their disregard may lead to interpretation pitfalls. These anisotropic effects can be modeled using Rüger reflectivity approximation for HTI media, described in terms of isotropic elastic properties and anisotropic Thomsen's parameters  $\epsilon^{(V)}$ ,  $\delta^{(V)}$  and  $\gamma$ . Therefore, we did a sensitivity analysis using a synthetic model with ISO-HTI and HTI-ISO interfaces, in order to evaluate and understand the anisotropy effects of Thomsen's parameters in the respective azimuthal AVO signatures.

## Introduction

As the wave propagation velocity depends on the direction in which the wave travels through the rock, the principal changes on seismic data, due anisotropy effects, are: different traveltimes of the reflected waves for each angle and azimuth, causing differential time shifts in the azimuthal gathers, and seismic amplitude variation with angle/offset when compared to isotropic case (Mesdag and Quevedo, 2017).

Since the anisotropy of rocks alters the seismic data signature, consider the anisotropic effects in the reservoir characterization allows a better understanding of several geological and geomechanical events in the subsurface.

The anisotropy of rocks can be categorized into intrinsic, e.g., the horizontal bedding of shales and the presence of natural fractures, or stress-induced anisotropy. The most common anisotropic models to describe these scenarios are the transverse isotropic (TI) models, characterized by a rotational symmetry axis with five independent components on the stiffness matrix (Schoenberg and Sayers, 1995; Rüger, 1998; Bakulin et al., 2000).

In order to study the azimuthal anisotropy observed in seismic data, the simplest TI media is the transversely isotropic model with a horizontal axis of rotational symmetry (HTI), frequently used to describe the effect of natural fracturing and in situ stress on the elastic behavior of rocks (Mavko et al., 1995; Gray et al., 2012).

To model these effects, Rüger (1997), following en (1993), derived a linearized approximation for P-P reflection coefficient in HTI media, assuming weak anisotropy and a boundary with small discontinuities in elastic properties. This approximation can be described by the isotropic elastic properties and the anisotropy Thomsen's parameters for an HTI media  $\epsilon^{(V)}$ ,  $\delta^{(V)}$  and  $\gamma$ , and has the same gradient term as the solution presented by Banik (1987) and Thomsen (1993), but is more accurate at larger angles.

In this work, we used the Rüger (1997) approximation for an HTI media to evaluate the AVO signatures on the top and bottom of the HTI layer in order to analyze the effects of the anisotropic Thomsen's parameters on the azimuthal AVO response. For this purpose, a synthetic model with two interfaces ISO-HTI and HTI-ISO was employed, as shown in Fig. 1.

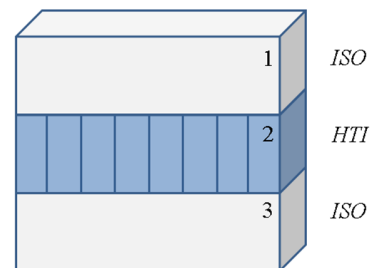


Figure 1: Synthetic model used to study the differences in the anisotropic AVO response. The model has an HTI layer embedded in an isotropic (ISO) medium.

## P-wave reflection coefficient for HTI media - Rüger (1997) approximation

HTI media is characterized by a horizontal axis of rotational symmetry and has two vertical symmetry planes: the plane formed by the symmetry axis, called symmetry-axis plane, and the plane perpendicular to the symmetry axis, called isotropy plane (Fig. 2). When the HTI symmetry is caused by a set of vertical fractures, the isotropy plane coincides with the fracture plane.

Waves travelling on the plane normal to the symmetry axis (isotropy plane) do not experience incidence angular velocity variation. However, for the others vertical planes

(including the symmetry-axis plane), the velocity changes with the incidence angle, complicating the interpretation of reflection data.

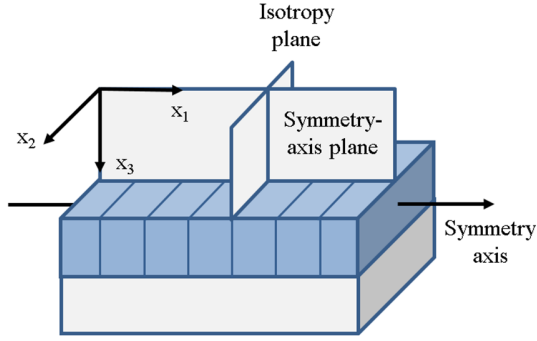


Figure 2: Sketch of an HTI model showing two vertical planes, the symmetry-axis plane and the isotropy plane.

As the shear waves propagating in the isotropy plane can travel with two different velocities, depending on whether their polarization is confined, to the isotropy plane or perpendicular to it, Rüger (1998) presented a linearized approximation for a P-P reflection coefficient in an interface between two HTI media with the same symmetry axis alignment for weak anisotropic case:

$$R_{PP}(i, \phi) = \frac{1}{2} \frac{\Delta Z}{Z} + \frac{1}{2} \left\{ \frac{\Delta \alpha}{\bar{\alpha}} - \left( \frac{2\bar{\beta}}{\bar{\alpha}} \right)^2 \frac{\Delta G}{\bar{G}} + \left[ \Delta \delta^{(V)} + 2 \left( \frac{2\bar{\beta}}{\bar{\alpha}} \right)^2 \Delta \gamma \right] \cos^2 \phi \right\} \sin^2 i + \frac{1}{2} \left\{ \frac{\Delta \alpha}{\bar{\alpha}} + \Delta \epsilon^{(V)} \cos^4 \phi + \Delta \delta^{(V)} \sin^2 \phi \cos^2 \phi \right\} \sin^2 i \tan^2 i, \quad (1)$$

where  $i$  denotes the incidence angle and  $\phi$  the azimuthal angle with the symmetry-axis plane. The  $\Delta$  indicates a difference and the overbar indicates an average of the corresponding properties across the boundary. The parameters  $\beta$  and  $\alpha$  are the isotropy-plane velocities of the fast vertical shear-wave (polarized parallel to the isotropy plane) and the vertical compressional wave, respectively:

$$\beta = \sqrt{\frac{c_{44}}{\rho}}, \quad (2)$$

$$\alpha = \sqrt{\frac{c_{33}}{\rho}}. \quad (3)$$

The parameter  $\rho$  represents the bulk density,  $G$  indicates the vertical shear modulus ( $G = \rho\beta^2$ ) and  $Z$  denotes vertical P-wave impedance ( $Z = \rho\alpha$ ),  $\epsilon^{(V)}$ ,  $\delta^{(V)}$  denote the anisotropic coefficients introduced by Rüger (1997), where the subscript  $^{(V)}$  symbolize the symmetric analogy assumption with Thomsen's (1986) parameters for VTI media and  $\gamma$  corresponds to the generic Thomsen's parameter defined with respect to the horizontal symmetry

axis. These parameters can be described in terms of elastic stiffness components  $c_{ij}$  (the  $c_{ij}$  representation corresponds to the symmetry axis pointing in the  $x_1$  direction in Fig. 2):

$$\epsilon^{(V)} = \frac{c_{11} - c_{33}}{2c_{33}}, \quad (4)$$

$$\delta^{(V)} = \frac{(c_{13} + c_{55})^2 - (c_{33} - c_{55})^2}{2c_{33}(c_{33} - c_{55})}, \quad (5)$$

$$\gamma = \frac{c_{44} - c_{66}}{2c_{66}}. \quad (6)$$

The anisotropic parameters  $\epsilon^{(V)}$  and  $\gamma$  denote the relative difference between vertical and horizontal compressional and shear velocities, respectively, and  $\delta^{(V)}$  describes the departure from isotropy for near vertical wave propagation.

According to equation (1), the parameters  $\delta^{(V)}$  and  $\gamma$  contribute to the reflection coefficient at lower angles (present in the term  $\sin^2 i$ ), while the  $\epsilon^{(V)}$  influences the higher incidence angles (present in the term  $\sin^2 i \tan^2 i$ ). For azimuth  $\phi = 90^\circ$ , we can state the approximate solution for the P-P reflection coefficient at the isotropy plane for HTI media, and the equation (1) reduces to:

$$R_{PP}^{iso}(i, 90^\circ) = \frac{1}{2} \frac{\Delta Z}{Z} + \frac{1}{2} \left\{ \frac{\Delta \alpha}{\bar{\alpha}} - \left( \frac{2\bar{\beta}}{\bar{\alpha}} \right)^2 \frac{\Delta G}{\bar{G}} \right\} \sin^2 i + \frac{1}{2} \frac{\Delta \alpha}{\bar{\alpha}} \sin^2 i \tan^2 i, \quad (7)$$

and for the symmetry-axis plane at azimuth  $\phi = 0^\circ$ , the reflection coefficient reduces to the following form:

$$R_{PP}^{ani}(i, 0^\circ) = \frac{1}{2} \frac{\Delta Z}{Z} + \frac{1}{2} \left\{ \frac{\Delta \alpha}{\bar{\alpha}} - \left( \frac{2\bar{\beta}}{\bar{\alpha}} \right)^2 \left( \frac{\Delta G}{\bar{G}} - 2\Delta \gamma \right) + \Delta \delta^{(V)} \right\} \sin^2 i + \frac{1}{2} \left( \frac{\Delta \alpha}{\bar{\alpha}} + \Delta \epsilon^{(V)} \right) \sin^2 i \tan^2 i. \quad (8)$$

The approximations described in equations (1), (7) and (8) are linearized in small, relative differences of the isotropic elastic properties and anisotropic Thomsen's parameters (useful assumption for inversion techniques), and are valid for incidence angles not too close to the critical angle (Rüger, 1998).

### Sensitivity analysis of P-wave reflectivity for HTI media

According to the synthetic model shown in Fig.1, the reflection coefficient was evaluated at boundaries of the HTI media (layer 2) considering four model parametrizations described in Table 1. For all cases, the isotropic elastic properties of the HTI media are:  $\alpha_2 = 2.5$  km/s,  $\beta_2 = 1.5$  km/s, and  $\rho_2 = 2.7$  g/cm<sup>3</sup>, and for the isotropic media (layer 1 and 3) are:  $\alpha_{1,3} = 2.26$  km/s,  $\beta_{1,3} = 1.43$  km/s, and  $\rho_{1,3} = 2.7$  g/cm<sup>3</sup>. The azimuth of the symmetry-axis/anisotropy plane for all models is  $30^\circ$ .

Table 1: The HTI medium Thomsen's parameters used to test the anisotropy sensitivity of reflection coefficients through equation (1).

Model	$\delta^{(V)}$	$\epsilon^{(V)}$	$\gamma$
1	-0.1	0	0
2	0	-0.1	0
3	-0.1	-0.1	0
4	0.1	0.1	0

The azimuthal seismic response was modeled using the convolutional model, where the reflectivity series were obtained from equation (1) for incidence angles up to 40 degrees approximately (~2000 m offset) and then convolved by a zero phase Ricker wavelet of 20 Hz central frequency. Figures 3 and 4 show, for each model, the seismic response for the azimuths 0°, 30°, 60°, 90°, 120° and 150°, which each azimuthal gather has five traces, e.g., the 0° azimuth gather is composed by 0-4 trace indexes, the 30° for 5-9 trace indexes, etc. The seismic response and the AVO signatures are also shown for both symmetry-axis/anisotropy plane (traces 5-9), and isotropy plane (traces 20-24) at the top and bottom of the HTI layer.

To study the compressional AVO reflection sensitivity with respect to the individual parameters, was selected negative and positive values for  $\delta^{(V)}$  and  $\epsilon^{(V)}$ , highlighting that for HTI media is expected negative values for these parameters (Hudson, 1988; Bakulin et al., 2000). During these tests, the generic  $\gamma$  Thomsen's parameter was fixed to zero. Rüger (1998) introduced positive values for this  $\gamma$  anisotropy parameter during his sensitivity studies following their proposed anisotropy reflectivity approximation model. For the  $\gamma^{(V)}$ , where  $^{(V)}$  symbolize the symmetric VTI analogy assumption, and is function of the generic  $\gamma$ , it is also expected negative values in an HTI media (Rüger, 1998; Bakulin et al., 2000).

Figure 3 and 4 show specifically the effects of  $\delta^{(V)}$  and  $\epsilon^{(V)}$  signals in the reflection signature. As expected,  $\delta^{(V)}$  in model 1 contributes to the departure between the reflection coefficients at isotropy and anisotropy planes for lower angles (present in the term  $\sin^2 i$ ), while the  $\epsilon^{(V)}$  in model 2 influences the departure for higher incidence angles (present in the term  $\sin^2 i \tan^2 i$ ). These models, in Fig. 3, show similar reflection signatures. In the Fig. 4, model 3 also shows a comparable trend with model 1 and 2, however, the departure is emphasized. In this model, the negative values of Thomsen's parameters can be associated with a fracture induced anisotropy environment. The model 4, with positive values of  $\delta^{(V)}$  and  $\epsilon^{(V)}$ , changes the reflection behavior giving opposite trends. These  $\delta^{(V)}$  and  $\epsilon^{(V)}$  Thomsen's parameters are more expected for a VTI medium, as related by Sayers (1994), Hornby et al. (2003), Walsh et al. (2007) and Jocker et al. (2013). This could explain the abrupt change of the reflection behavior, when compared to the other models conditioned for an HTI media. The assumptions described above can be evaluated for both ISO-HTI and HTI-ISO interfaces.

## Conclusions and recommendations

To study the anisotropy reflection sensitivity was selected negative and positive values for  $\delta^{(V)}$  and  $\epsilon^{(V)}$  and fixing zero for  $\gamma$  in order to analyze the influence of these anisotropic parameters in the AVO signatures for short and long offsets at different azimuths.

It was proved that  $\delta^{(V)}$  and  $\epsilon^{(V)}$  individually contribute to the AVO signature departure between symmetry/anisotropy and isotropy planes for lower and higher incidence angles, respectively. These effects are observed at ISO-HTI and HTI-ISO interfaces and are emphasized when both  $\delta^{(V)}$  and  $\epsilon^{(V)}$  are considered in the Rüger approximation. Thus, disregard the anisotropic parameters can lead to interpretation pitfalls since the AVO signature has a considerable sensitivity when anisotropy is present.

The understanding of the anisotropy effects in reflection responses can be extended for other advanced analysis linked with physical and geomechanical properties through rock physics models (Schoenberg and Sayers, 1995; Hudson, 1988). These models correlate the anisotropic Thomsen's parameters with reservoir properties, as fluid content, crack density and fracture compliance.

It is recommended to include a  $\gamma$  parameter sensitivity study in the future, considering uncertainties related to shear splitting phenomenon modeling, as well as the importance of this parameter for fracture characterization (close to crack density).

## Acknowledgments

We thank ANP and Queiroz Galvão Exploration and Production for support this project.

## References

- Bakulin, A., Grechka, V., and Tsvankin, I., 2000, Estimation of fracture parameters from reflection seismic data - Part I: HTI model due to a single fracture set: *Geophysics*, 65, 1788-1802.
- Banik, N. C., 1987, An effective anisotropy parameter in transversely isotropic media: *Geophysics*, 52, 1654-1664.
- Gray, D., Anderson, P., Logel, J., Delbecq, F., Schmidt, D., and Schmid, R., 2012, Estimation of stress and geomechanical properties using 3D seismic data: *First Break*, 30, 59-68.
- Hornby, B., Howie, J., and Ince, D., 2003, Anisotropy correction for deviated-well sonic logs: application to seismic well tie: *Geophysics*, 68, 464-471.
- Hudson, J. A., 1988, Seismic wave propagation through material containing partially saturated cracks: *Geophysics*, 92, 33-37.

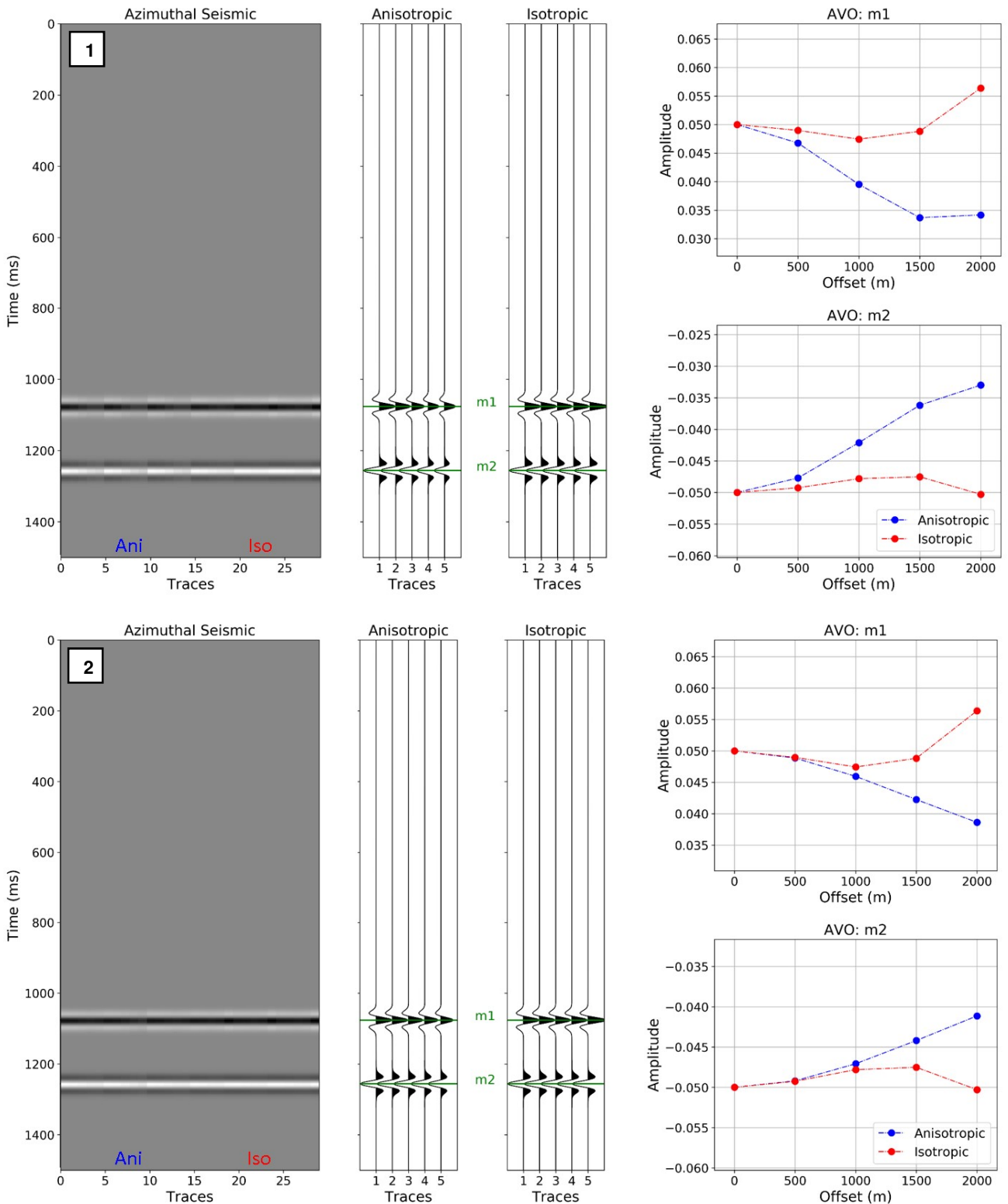


Figure 3: Reflection coefficient panel for an HTI layer embedded in an isotropic medium for models 1 (top) and 2 (bottom), described in Table 1. From left to right are: the azimuthal seismic response modeled for 6 azimuths (0°, 30°, 60°, 90°, 120°, 150°) with 5 traces each, e.g., the 0° azimuth gather is composed by 0-4 trace indexes, the 30° for 5-9 trace indexes, etc; the seismic gathers for the anisotropy/symmetry-axis (30° azimuth) and isotropy (120° azimuth) planes; and the AVO response at ISO-HTI ( $m_1$  marker) and HTI-ISO ( $m_2$  marker) interfaces for anisotropy and isotropy planes.

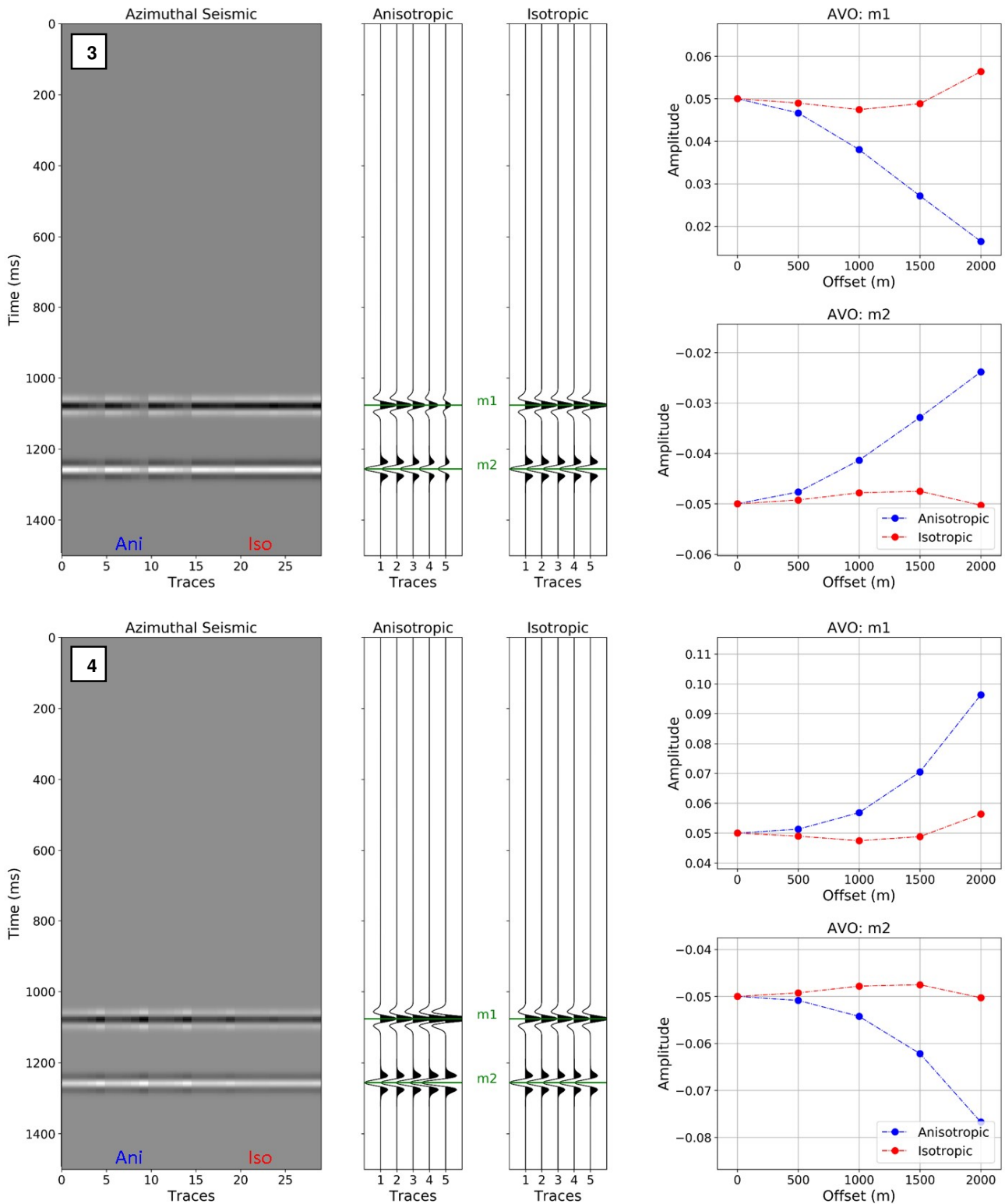


Figure 4: Reflection coefficient panel for an HTI layer embedded in an isotropic medium for models 3 (top) and 4 (bottom), described in Table 1. From left to right are: the azimuthal seismic response modeled for 6 azimuths ( $0^\circ$ ,  $30^\circ$ ,  $60^\circ$ ,  $90^\circ$ ,  $120^\circ$ ,  $150^\circ$ ) with 5 traces each, e.g., the  $0^\circ$  azimuth gather is composed by 0-4 trace indexes, the  $30^\circ$  for 5-9 trace indexes, etc; the seismic gathers for the anisotropy/symmetry-axis ( $30^\circ$  azimuth) and isotropy ( $120^\circ$  azimuth) planes; and the AVO response at ISO-HTI ( $m_1$  marker) and HTI-ISO ( $m_2$  marker) interfaces for anisotropy and isotropy planes.

Jocker, J., Ferla, M., Pampuri, F., and Wielemaker, E., 2013, Seismic anisotropy characterization in heterogeneous formations using borehole sonic data: 75th EAGE Conference & Exhibition.

Mavko, G., Mukerji, T., and Godfrey, N., 1995, Predicting stress-induced velocity anisotropy in rocks: *Geophysics*, 60, 1081-1087.

Mesdag, P. R., and Quevedo, L., 2017, Quantitative inversion of azimuthal anisotropy parameters from isotropic techniques: *The Leading Edge*, 36, 916-923.

Rüger, A., 1997, P-wave reflection coefficients for transversely isotropic models with vertical and horizontal axis of symmetry: *Geophysics*, 62, 713-722.

Rüger, A., 1998, Variation of P-wave reflectivity with offset and azimuth in anisotropic media: *Geophysics*, 63, 935-947.

Sayers, C. M., 1994, The elastic anisotropy of shales: *J. Geophys. Res.*, 99, 767-774.

Schoenberg, M., and Sayers, C. M., 1995, Seismic anisotropy of fractured rocks: *Geophysics*, 60, 204-211.

Thomsen, L., 1986, Weak elastic anisotropy: *Geophysics*, 51, 1954-1966.

Thomsen, L., 1993, Weak anisotropic reflections, in *Offset dependent reflectivity*, Castagna, J., and Backus, M., Eds: *Soc. Expl. Geophys.*, 103-114.

Walsh, J., Sinha, B., Plona, T., and Miller, D., 2007, Derivation of anisotropy parameters in a shale using borehole sonic data, in *SEG Annual Meeting, Expanded Abstracts*, 26, 323-327.